Volume 65, Issue 3, 2021
Journal of Scientific Research
Institute of Science,
Banaras Hindu University, Varanasi, India.

Evaluation of Active Tectonics and Geomorphic Indices in Siwalik Basin Around Dikrong River, Eastern Himalaya

Archana Singh* and Devojit Bezbaruah

Department of Applied Geology, Dibrugarh University.
itsarchana.singh456@gmail.com*, devojit.bezbaruah@gmail.com

Abstract: **The Eastern Himalaya region is a comple * x combination of two events: (a) collision between the Indian and Eurasian plates and (b) erosional and depositional processes occurring in the area. The study area is a part of Sub-Himalaya, which comprises the Siwalik Group of rocks. The present study includes the Dikrong River, which has a vast valley of about 4-5 km, and there is an offset in the mountain front on both sides of the river. The presence of horizontal and tilted terraces and uplifted rock formations provide an excellent set up to study the degree of tectonic activity. Geomorphic indices used to fulfil the objective are stream-length gradient, Mountain front sinuosity, valley floor width to valley height ratio, asymmetry factor. In this paper, we have discussed the results of the geomorphic indices and also the evidence of active tectonic activity. Also, we have discussed the cause of negative indication of few geomorphic indexes, which indicates the area to be less active. It is known from the tectonic evidence that the region is tectonically very active. A new set of data range of tectonic activity classes with particular reference to the Eastern Himalayas is required to eliminate the error in the results.**

Index Terms: **Active tectonics, Geomorphic Indices, Eastern Himalaya, Dikrong River, Siwalik.**

I. INTRODUCTION

Geomorphic indices are particularly useful in the active tectonic evaluation as they can provide a prompt understanding of the concerned area undergoing relatively rapid or even tectonic adjustment (Keller, 1986). One of the emergent disciplines in Earth science is active tectonics. It is a new tool facilitating the acquisition of rates (uplift and incision rate, erosion rate) after the progress of geochronological and geodetic methods (Schumm et al., 2000; Burbank & Anderson, 2001; Keller & Pinter, 2002; Bull, 2007). Geomorphic indices are employed to investigate the degree of tectonic activity. These indices offer a quantitative approach to the geomorphic analysis related to erosional and deposition processes. Such processes include channel morphology, longitudinal profile, valley morphology and features derived tectonically like terraces and fault scarps. Geomorphic indices detect the anomalies in the drainage basin or mountain fronts produced by tectonic activities like upliftment or subsidence occurring in the area (El Hamdouni et al., 2008).

Geomorphic index application helps in extracting necessary information in the areas experiencing deformation in terms of active tectonics. It explains the cause of the evolution of a particular landscape (Bull, 1977b, Bull & McFadden, 1977; Keller & Pinter, 2002; Zovoili et al., 2004). Recent and active tectonics in the mountain ranges is the dominant component contributing to uplift of rocks. The present-day topography of the mountain ranges is the evolved product of an interaction between tectonic activities and erosional processes (England & Molnar, 1990; Bishop 2007; Perez-Pena et al., 2010). Tectonic processes such as folding and faulting affect the drainage pattern and led to phenomena such as accelerated river incision, river diversions and asymmetries in the catchment (Cox, 1994; Jackson et al., 1998; Perez-Pena et al., 2010). The recent and present-day tectonic activity can be applied to assess topography, drainage pattern and geomorphic features (Keller et al., 2000; Azor et al., 2002; Perez-Pena et al., 2010). In such studies, data required for evaluation can be derived from DEM, aerial photographs and topographic maps.

* Corresponding Author

II. GEOLOGICAL AND NEOTECTONIC SETTING

The present study area (Fig. 1) lies in the Himalayan foredeep located in the northern side of the Indian Plate. The area has numerous tectonic signatures because of its location in the thrust since the time of the collision, although its rate has fluctuated during its journey. The Indian plate is continuing to converge at a rate of 5 cm/year (Patriat & Achache, 1984). (Chatterjee et al., 2013). It has led to the ongoing development of a series of

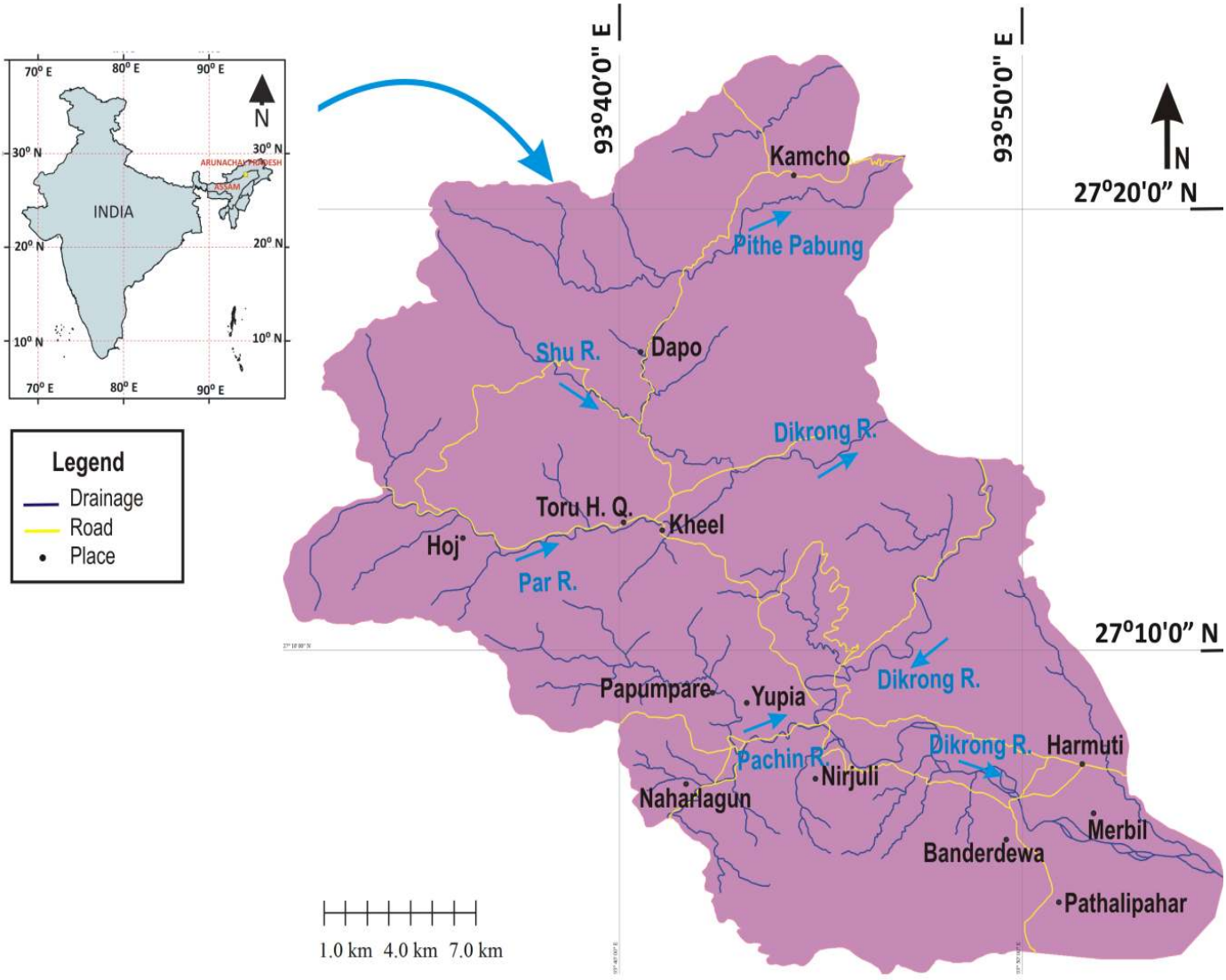

Figure 1: Location map of the study area.

zone. It is present in the border areas of Assam and Arunachal Pradesh. The study area includes Papumpare district of Arunachal Pradesh and North-Lakhimpur district of Assam, bounded between longitude 93º 31' E to 93º 55' E and latitude 27º 24' N to 27º 01' N. The area lies between the Main Boundary Thrust (MBT) in the north and the Himalayan Frontal Fault-3 (HFT 3) in the south. The study area has four thrusts and one prominent strike-slip fault, known as Banderdewa fault. Major thrusts from north to south are MBT, HFT 1, HFT 2 and HFT 3. These thrusts, landscapes in the region and many other deformational structures formed due to the collision between the Indian plate and Eurasian plate. This collision started at early Eocene (~50 Ma) and led to the formation of the Himalayan orogenic belt. The convergence of these plates is still in progress thrusts in the Himalaya following crustal shortening of approximately 2500 km (Patriat & Achache, 1984). There is a regular and balanced southward progression of thrust faulting, Indus–Tsangpo Suture (ITS) from the north and following after, the Main Central Thrust (MCT), the MBT, and the HFT formed farther in the south (Allègre, 1984). The MBT is a sequence of thrust splays. These thrust splays divide the sediments of pre-tertiary Lesser Himalaya from the sedimentary belt of Tertiary Siwalik. The Sub-Himalaya which lies in the foothills of the Himalaya lies in the south of Lesser Himalaya and has an average height of 900m to 1200m. The Sub-Himalaya mountain range covers a vast area in terms of width, ranging from 8 to 80 km. Lesser Himalaya over-thrusted Sub-Himalaya along the

MBT and Sub-Himalaya thrust over alluvium along the HFT (Chatterjee et al., 2013).

The study area (Fig. 2) lies in the Sub-Himalayan region of Arunachal Pradesh and consists of the Siwalik Formation. According to the stratigraphy and structure proposed by Karunakaran and Rangarao (1979) in their works with ONGC, the Siwaliks in Arunachal Pradesh has three subdivisions. These three subdivisions are Dafla, Subansiri and Kimin Formation.

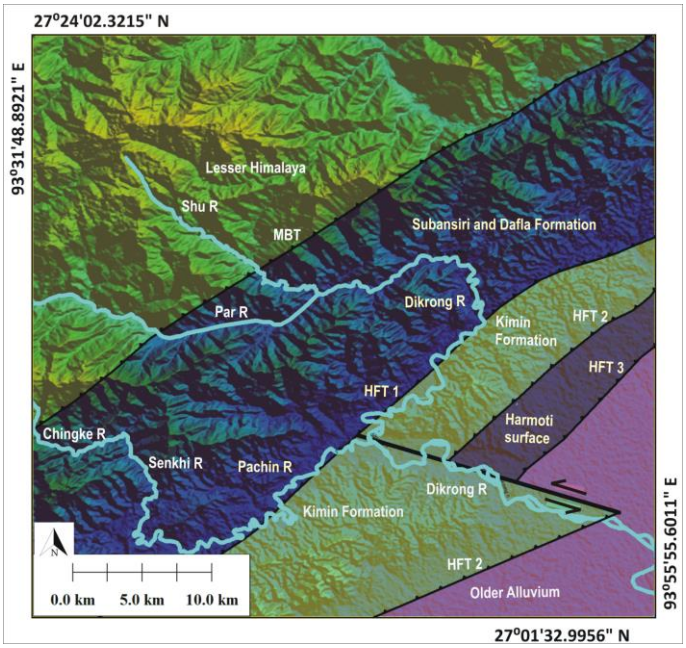

Figure 2: Geological map showing major thrust and rock formation present in the area. The major river flowing in the region is Dikrong, Pachin, Shu and Par River.

The Kimin Formation is youngest among them, while the oldest is Dafla Formation. The Dafla Formation consists of alternate beds of indurated fine-grained sandstone, greenish-grey claystone, shale and the rare occurrence of thin lenses of coal. The Dafla Formation is thrusted over Subansiri Formation by the Tipi Thrust, which lies between MBT and HFT. The Subansiri Formation consists of soft, coarser-grained massive sandstone having salt and pepper texture that resembles the Middle Siwalik (Ranga Rao, 1983). The youngest of the Tertiary formations is the Kimin Formation and is consist of conglomerates, pebble beds with sandy matrix in sandstone with alternations of soft, current-bedded sandstone, siltstone, clays and gravels (Ranga Rao, 1983; Kunte et al., 1983). The lithology in the study area comprises the Kimin Formation, which is thrusted over the alluvial plain by HFT. The HFT in this region has branched out into several thrust splays. These splays from HFT separates the sedimentary deposits of the Siwalik Group from the quaternary deposits of alluvium. The splays of HFT in the present area from north to south are HFT 1 which has thrusted the Subansiri Formation over the Kimin Formation, HFT 2 over-thrusted the Kimin Formation over the Harmoti Surface in the East bank of Dikrong River and the Harmoti surface is over-thrusted over Older Alluvium deposits by HFT 3. As mentioned earlier, the area has a strike-slip fault known as Banderdewa Fault, along which the Dikrong River flows (Devi et al., 2011). The Dikrong river valley which is approximately 4 km wide is a pull-apart basin. The basin is undergoing differential compression in its east and west bank. The upliftment and denudation process explains all the geomorphological development. The additional factors playing a vital role in the process are lithology and climate of the zone.

III. METHODOLOGY

The geological features in the area are mapped in detail and digitized using Aster-GDEM of 30m resolution, Survey of India toposheets and field investigations. Geological structures in the map show distinct properties concerning slope, elevation, contour pattern and relief. It allows identification of features through satellite images, DEM and Toposheets. The geological structures such as faults, folds, terrace deposits and uplifted bedrocks are recorded in the field investigations. The drainage basins are identified as 3rd, 4th, 5th and 6th order as per the Strahler's stream order method. The drainage basins are sensitive to the degree of tectonic activity and their shape, size and relief rely on tectonic deformation and other erosional and denudational processes. The stream network develops geometries and distinctive patterns which can be interpreted qualitatively and quantitatively (Hare & Gardner, 1985; Keller & Pinter, 2002).

The geomorphic indices employed are Mountain Front Sinuosity (Smf), Valley floor width to valley height ratio (Vf), Mountain front steepness index (S), Asymmetry factor (Af), Transverse topographic symmetry factor (T), Basin shape index (Bs) and Stream length gradient index (SL). We divide the area for the research into three sections, i.e., 1, 2 and 3. The major thrust present in the study area is bounding the sections. Section 1 is the study area lying above MBT, between MBT and HFT-1 is section 2 and section 3 is the study area below HFT-1.

A. Mountain front sinuosity

It is defined by the formula (Bull & McFadden, 1977; Bull, 1978)

Smf = Lmf / Ls

Where Lmf is the length of the mountain front measured at its base where there is a distinct break in slope and Ls is the straight length of the mountain front. The mountain front sinuosity index expresses the balance between the process of stream erosion and active vertical tectonics. The stream erosion erodes some parts of mountain fronts, whereas active vertical tectonics is responsible for straight mountain fronts (Bull & McFadden, 1977; Keller, 1986).

B. Valley floor width to valley height ratio

This index makes a distinction between V-shaped and U-shaped Valleys and relates its association with active tectonics. It is computed by formula (Bull & McFadden, 1977)

VF = 2Vfw/ (Eld+Erd-2Esc)

Where Vfw is the valley floor width, Eld and Erd are the elevations on the left and right side of the valleys, Esc is the valley floor elevation (Fig. 3).

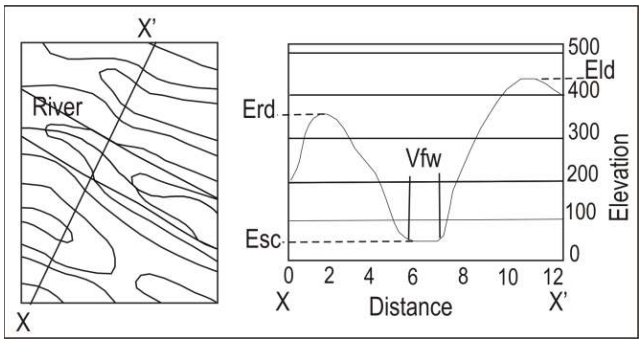

Figure 3: Representative diagram for measuring VF. (From Keller & Pinter 2002, fig. 4.15, p. 139).

The V-shaped valleys are narrow, steep and have lower Vf values suggestive of active tectonics. The U-shaped valleys have wide floor relative to height and have high Vf values, which is indicative of less tectonic influence in the area.

C. Asymmetry factor

The asymmetry factor (Af) helps in identifying tectonic tilting. The measurements are on the scale of a drainage basin. Its application is also possible over a relatively huge area (Hamdouni et al., 2008; Hare & Gardner, 1985; Keller & Pinter, 2002). AF is defined by

$AF = (A_r/A_t) \times 100$

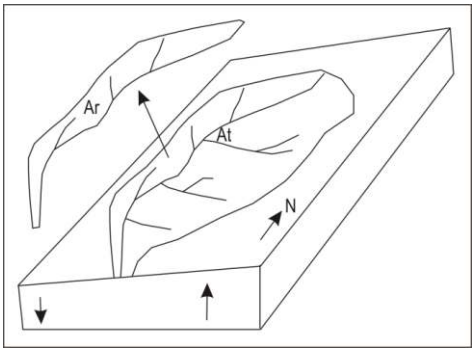

Figure 4: Representative diagram for AF calculation. (Modified from Keller and Pinter 2002, figure 4.3, p. 125).

Where A_r is the area of the basin to the right of the trunk stream (facing downstream) and A_t is the total drainage basin area (Fig. 4).

D. Transverse Topographic Symmetry Factor

T evaluates asymmetry and indicates the tilting direction of the basin by considering the shift of trunk stream from the basin midline. It is defined as

$T = D_a/D_d$

Where D_a is the distance between the midline of basin to the trunk stream and D_d is the distance between drainage basin midline to basin divide (Fig. 5).

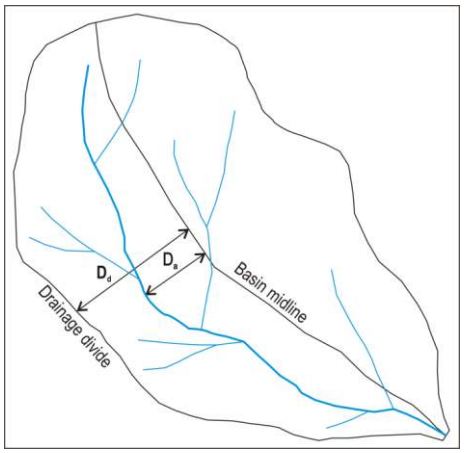

Figure 5: Representative diagram for Transverse topographic symmetry factor calculation. (From Cox 1994, figure 3, p. 574).

E. Basin shape index

The drainage basins in a tectonically active mountain range are elongate, and after the halt of mountain uplift, the basin attains a circular shape progressively with time (Bull & McFadden, 1977). Thus, the planimetric shape of a basin defines the Basin Shape Index (Cannon, 1976; Ramírez-Herrera, 1998).

Bs=Bl / Bw

Where Bl is the length measured from the mouth of the basin to the farthest drainage divide, and Bw is the basin width measured at its widest point (Fig. 6).

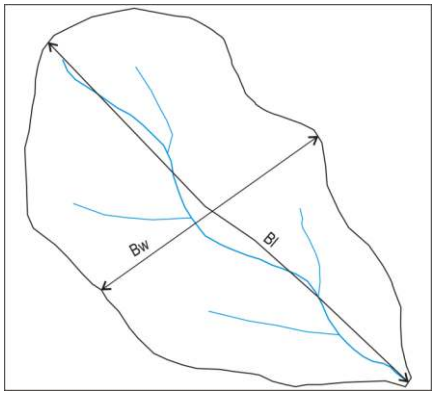

Figure 6: Representative diagram for calculation of Basin shape index. (Modified from Burbank and Anderson 2001, figure 10.2, p. 203).

F. Mountain front steepness index

The Mountain front steepness index helps in identifying the change in topography from hill to plane in frontal parts of the mountainous ranges. Topography in mountainous regions changes abruptly from hills to plane in frontal portion. The index is measured by taking cross profile of the mountain front, which are extracted from DEM. A tectonically active will have a

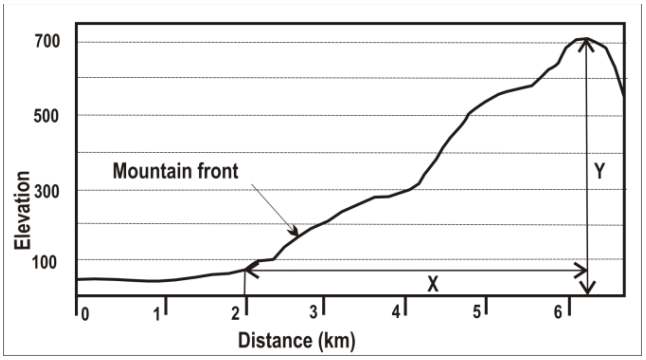

Figure 7: Representative diagram for mountain front steepness index calculation.

steeper mountain front compared to less active mountain front, given the lithology, climate and vegetation of the region is uniform. The steepness of the mountain front depends on many elements such as rock strength, climate and vegetation, also whether its front is adjusted to the pattern of threshold hill slope or it is still in a transient state. Therefore, we attempted to introduce an index which is the mountain front steepness index. Mountain front steepness is computed by formula

$Ms = Y/X$

Where X is the horizontal distance between the hill to the plane where sharp changes in slope occur, and Y is the vertical distance between the highest elevation points of the hill down to the point where the slope breaks (Fig. 7).

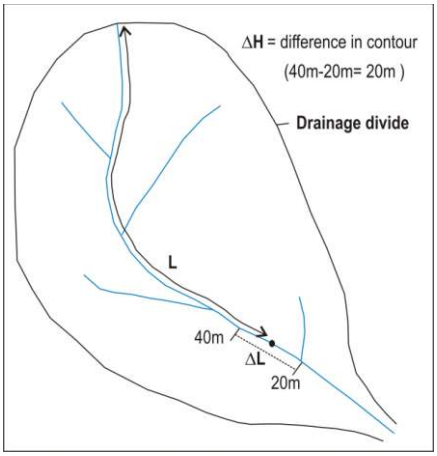

Figure 8: Representative diagram for Stream length gradient index calculation. (From Keller and Pinter 2002, figure, 4.6, p. 128).

G. Stream Length Gradient Index

SL index is employed to find any deviation in the stable river longitudinal profile, which may be influenced by tectonic, climatic factors or lithology in the area (Hack, 1973). It is defined by Hack (1973) as

$SL = (\Delta H/\Delta L)\ L$

Where $\Delta H/\Delta L$ is the channel slope, ΔH is the elevation change, ΔL is the length of the reach, and L is the channel length between the midpoints of the reach to the divide (Fig. 8).

IV. RESULTS

Eighty-one basins, sub-basins and mountain fronts are dealt with in the area around Dikrong River (Fig. 9) for determining the degree of tectonic activity in the study area. The sub-headings in this section discusses the result of each index.

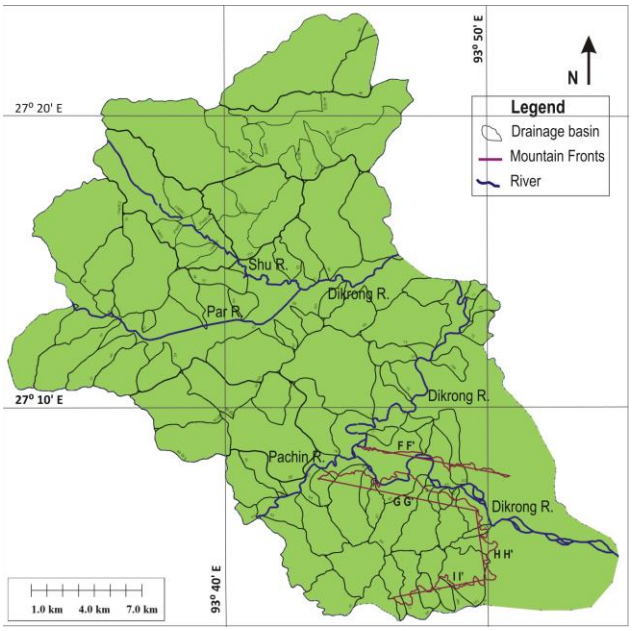

Figure 9: Drainage basins around Dikrong River and adjacent area present in the area. Major rivers and four mountain fronts taken into study are marked in the map.

A. Mountain front sinuosity

The Smf is calculated at fronts F F', G G', H H' and I I' out of which, F F' and G G', lies along the banks of Dikrong River which is the trend of Banderdewa Strike-slip fault. There is a classification of tectonic activity classes given by Bull & Mcfadden, 1977; Rockwell et al., 1984; Silva et al., 2003 (Table I). It is obtained that the fronts F F' and G G' fall under 1 (active) and 1 to 2 tectonic classes (Table II), indicating activeness on both sides of the river bank. It is also the location of the Banderdewa Fault (strike-slip). The fronts H H' and I I' fall in the 2nd class of tectonic activity and suggest a moderate tectonic activity occurring in the area. The terrain comprises friable sedimentary rocks and conglomeratic beds of the Kimin

Formation. Hence, it is a probability that the results are affected by climatic conditions and lithology of the study area.

Table I: Range of tectonic activity classes given by different authors.

Authors	Tectonic classes	Smf ranges	Vf ranges
Bull & Mcfadden(1977)	1	1.0 to 1.6	0.05-0.9
	2	1.4 to 3.0	0.5- 2.0
	3	1.5 to >5	>2.0
Rockwell et al. (1984)	active fronts	1.01- 1.34	0.43-1.91
	less active fronts	1.57- 2.72	
Silva et al. (2003)	1	1.17- 1.53	<0.5
	2	1.8- 2.30	0.3-0.8
	3	2.8- 3.5	>0.7(mostly 0.8-1.2)

Table II: The Smf values obtained for the fronts and their tectonic activity class.

Front	Smf (avg)	Tectonic activity class		
		Bull & Mcfadden(1977)	Silva (2003)	Rockwell (1984)
F F'	1.277	1	1	1 to 2
G G'	1.373	1	1	1 to 2
H H'	1.878	2	2	2
I I'	1.714	2	2	2

B. Valley floor width to valley height ratio

We calculate the Vf for third and higher order basins. The transect distance for the valley profiles is taken at two points upstream from the mountain fronts, one at 300m (Silva et al., 2003) and another at 1 km (Bull & McFadden, 1977). It is taken at two point to analyze and compare the result concerning upliftment, incision and erosion. The VF is calculated for three fronts excluding H H' as there are no major drainage basins along this front. The VF obtained at transect distance 300m is moderately active for I I' and inactive for F F' and G G'. At 1 km distance, G G' is active and VF for F F' and I I' front is moderately active (Table III).

Table III: The Vf mean value for the fronts and their tectonic activity class.

Distance	Front	Vf mean	Class
300 mt	F F'	0.993	3
	G G'	1.135	3
	I I'	0.507	2
1 km	F F'	1.25	2
	G G'	0.705	1
	I I'	1.086	2

C. Asymmetry factor

The Af for the basins varies from symmetric to strongly asymmetric nature. In the present study, Af is expressed as an absolute value. It is the difference between the observed value of Af and 50 (Absolute Af = Observed Af–50). The Af equals 50 indicates a stable condition. The absolute Af have four classes based on absolute Af values: Af < 5 (class 1, symmetric basins), Af = 5-10 (class 2, gently asymmetric basins), Af = 10-15 (class 3, moderately asymmetric basins), and Af > 15 (class 4, strongly asymmetric basins) (Perez Pena et al., 2010). Different classes of Af for the drainage basins in the area are present on the map. The titling directions of the basins are towards the pointing direction of the arrow (Fig. 10). We find that 15 basins are symmetrical, and 28 basins are highly asymmetrical. In some case, even highly asymmetrical basin with larger drainage area falls in class 1 Af. The cause behind this deviation is the two opposite tilting direction within the same basin, such as one part tilting in the NW direction and the other part in SE. This effect could present even a highly asymmetrical basin to the symmetrical category by directly following the AF formula. The presence of tilting and asymmetry in most of the basins indicates ongoing tectonic activity.

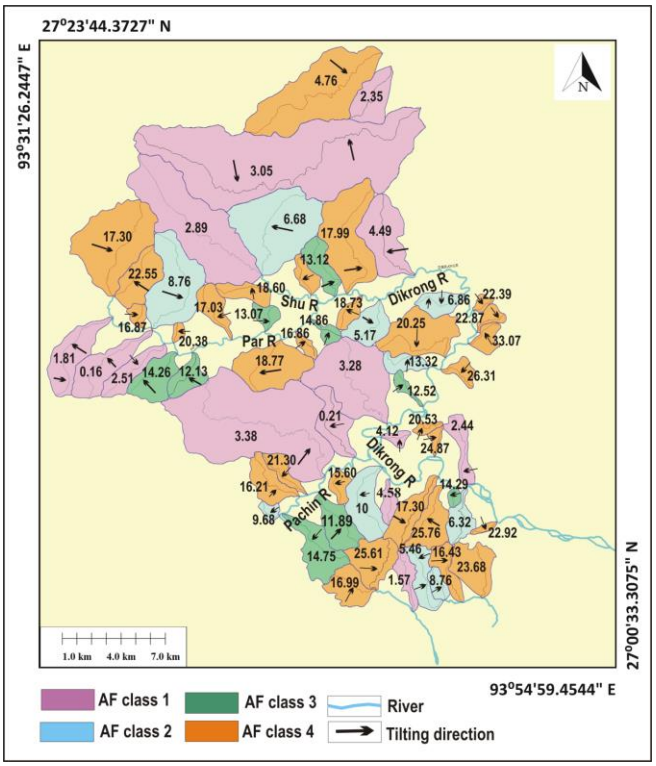

Figure 10: Asymmetry map of the area. The black arrow within the basin is pointing towards the tilting direction of the basin.

D. Transverse Topographic Symmetry Factor

On examining the general trend of the active meander belt of the basins, we observed that the course of the main channel for the basins above MBT is towards the SW and NW direction. It is

in the SW direction for basins between the MBT and HFT and towards E and W directions for the basins below HFT. (Table IV). The maximum value of T is ranging from 0.65 to 0.68 and indicates high active tectonic activity. The asymmetry of the basin increases as the T value approaches 1. The tilting of the basin in a particular direction brings changes in its slope component. It led the stream to change its course and shift towards the tilting direction, increasing the length of tributaries.

Table IV: T values of the basins and dominant tilting directions in three divided segments of the study area.

Divisions	Dominant tilting direction	T values
Below MBT	SW and NW	0.136 - 0.627
Between MBT and HFT	SW	0.192 - 0.68
Below HFT	E and W	0.266 - 0.651

E. Basin shape index

The basin shape index is calculated for all the basins and categorized into three classes (Table V). The Bs value for the basins above MBT is from 0.74 to 3.80, where out of 37 basins, 6 are semi-circular, and the rest are circular. The Bs is 1.15 to 3.06 for basins between MBT and HFT-1, where 1 out of 20 basins is semi-circular, and the rest are circular. The values for the basins below HFT-1 are 0.99 to 3.64, where only 4 out of 20 basins are semi-circular, and the rest are circular. Most of the basin in the study area is circular. The basins lying between MBT and HFT-1 are semi-circular.

Table V: Classes of Basin shape index (El Hamdouni et al., 2008)

Class	Range	Shape
1	$Bs \geq 4$	Elongated
2	$4 \geq Bs \leq 3$	Semi circular
3	$Bs \leq 3$	Circular

F. Mountain front steepness index

In the present study, the mountain front steepness index is calculated by taking cross-sections perpendicular to the mountain fronts H H' and I I' and cut summit of the mountain close to the mountain front. The value obtained is 0.309 for the front H H' and 0.169 for I I', clearly inferring that the segment I I' is more active than the segment H H'.

G. Stream Length Index

We measure the SL index in the study area for the basin of a third or higher order. The graphs for the SL study are made by plotting SL values against distance from the source to the point of measurement in the river profile (Fig. 11). The high and low anomalous points are marked and shown on the map. (Fig. 12).

There is a wide spatial distribution of anomalous SL high and low values in the study area. Anomalous points are in alignment with the major fault zone. A high number of anomalous SL points lie in the zone above MBT and between MBT and HFT-1. The area between the MBT and HFT-1 comprises of the Subansiri and Dafla Formation and is composed of friable and easily erodible soft rocks. The soft lithology may be responsible for numerous high and low anomalous points in the area. The yellow points in the map (Fig. 12) represent high SL values. They are place of confluence of the lower order stream with higher order stream. The higher order streams have high discharge, sediment load, and erosional capacity. So, when a stream of lower order meets a higher order stream at a point, it forms a spot of local steepness. So, we are getting high SL values in the points of confluences.

If the SL index is analyzed in the context of rock strength, the rocks above MBT, which comparatively have higher rock strength, have more high anomalous SL points. It clearly indicates the dominance of the tectonic process in the area.

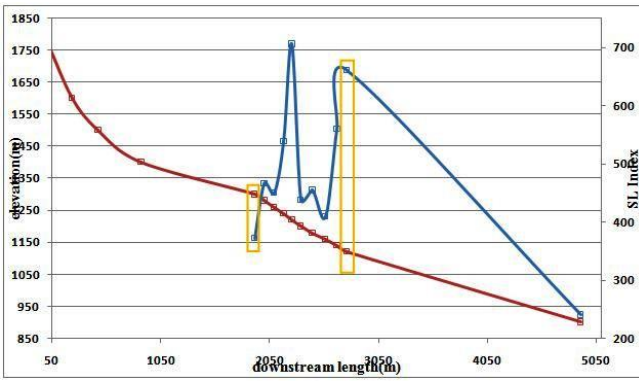

Figure 11: SL graph and longitudinal profile of Lumchi Pabung basin which lies above MBT. The knick point in the SL graph and longitudinal profile is marked within yellow square box.

H. Relative tectonic activity (IRAT)

Previous studies in approach to provide information about the relative degree of tectonic activity used two indices (Smf and VF). Using these two indices, they assigned different tectonic activity classes (Bull & McFadden, 1977; Silva et al., 2003). These methods focused on the active tectonic assessment along the mountain fronts and not on the regional appraisal of active tectonics (El Hamdouni et al., 2008). For the regional assessment of active tectonics, El Hamdouni, 2008 developed Irat by taking an average of the different classes of geomorphic indices. It has four categories of tectonic activity where Irat value between 1 and 1.5 is a class 1 (very high tectonic activity); class 2 is 1.5 to 2 (high tectonic activity); class 3 is 2 to 2.5 (moderately active tectonics), and class 4 values more than 2.5 (low active tectonics). Irat in the study area is calculated by taking all the parameters (Table VI). Since we have calculated

VF at two transect distance, Irat is calculated separately for both VF while it includes all the other indices.

Table VI: Irat values and classes for three segments taking average of all the parameters (two separate Irat values and classes are shown for two transect distance of VF).

	For VF values at 1km		For VF values at 300mt	
Segment	Irat value	Irat class	Irat value	Irat class
Basins above MBT	3.053	4	3.053	4
Between MBT and HFT 1	3.348	4	3.348	4
Basins below HFT 1	3.381	4	2.364	3

Table VII: Irat values and classes by taking only two indexes (AF and SL).

Segment	IAT value	IAT class
Basins above MBT	1.842	2
Between MBT and HFT 1	1.913	2
Basins below HFT 1	1.881	2

The Irat results in both cases are showing low tectonic activity (class 4) in the area. The Irat is obtained by taking five parameters that are Smf, Vf, Af, Bs and SL index. Smf, Vf and Bs shows the region to be lesser active. The friable and erodible rock character and heavy precipitation in the study area alter the topography. It makes the mountain front more sinuous and valley wider. Gradually the basin becomes circular at a faster rate because of high head ward erosion. So, we have attempted

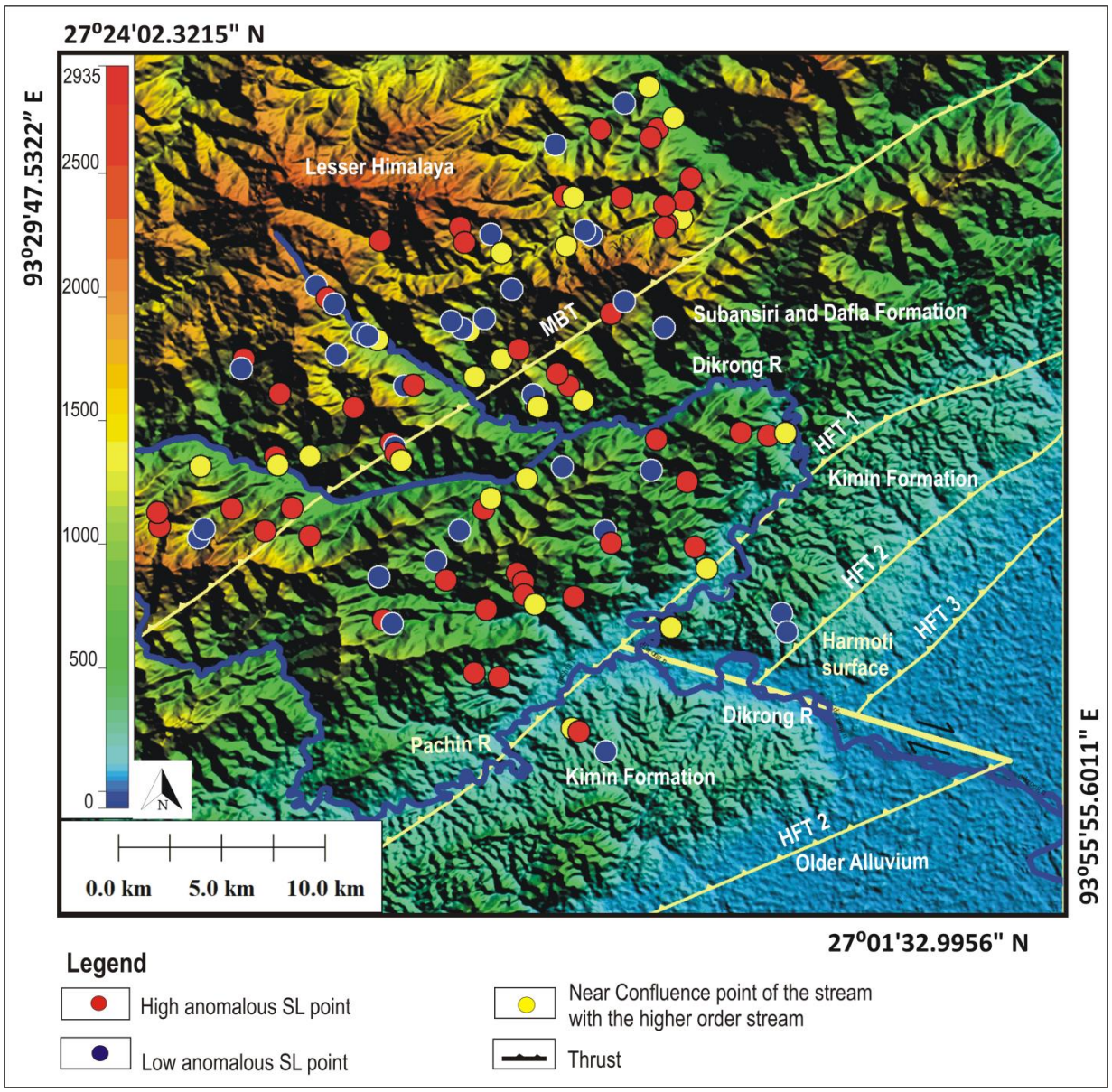

Figure 12: SL map of the study area showing clusters of anomalous points in the region.

to calculate Irat taking parameters that are showing the area as active to have a comparative overview. The Irat obtained on including AF and SL is class 2, showing high tectonic activity (Table VII). The study shows that for calculating Irat in the area with easily erodible rocks and heavy precipitation, we must use Af and SL instead of Smf, Vf and Bs.

V. EVIDENCES OF ACTIVE TECTONICS

The tilted terraces of several levels in the study area express recent tectonic activity. The tilted terrace deposits at many locations have small scale faults and folds (Fig. 13). Presence of three splays of HFT in the East bank and two splays in the west bank (Fig. 2). Deformation of terrace deposits of early Quaternary Period and overriding of these deposits above recent alluvium along HFT-3 in the East bank. Offset of mountain front along Banderdewa fault (Fig. 2). These are all pieces of evidences of active tectonics in the study area. Further presence of the strath terrace with thick alluvium cover indicates ongoing tectonic activity (Fig. 14).

In the Dikrong river section, the foredeep where the Siwaliks deposited is formed probably during the early Miocene because of the overriding of thrust sheets. With further compression in the foreland basin, HFT 1 developed, which is clear from the boulders of the Subansiri Formation present within the Kimin Formation (Fig. 15). It shows that the Subansiri Formation was uplifted during the Kimin Formation deposition and became a source for the Kimin Formation. The continued compression resulted in the HFT-2 development in the south of HFT-1, and the Kimin Formation thrusted over the recent alluvium. The Kimin beds have a steeper disposition in the east bank and gentler on the west bank of the Dikrong river. This difference is due to the differential resistance during the propagation of the thrust sheet. This differential strain on both banks is accommodated by the strike-slip fault forming a vast valley along which the Dikrong River is flowing. The Harmati surface present in the south of HFT 2 rises above recent alluvium along HFT-3. The terrace deposits in its south have a horizontal disposition while it tilts in the northern part near Ghola-Juli (Fig. 16) (Bezbaruah and Sharma, 2013). The strike slip fault has caused an offset in the mountain front along the Dikrong river valley.

VI. DISCUSSION

Along with the shreds of evidence supporting the tectonic activeness of the area, the geomorphic evidence further proves and provides a degree of tectonic activity. The region has a very high precipitation range (2700-4300 mm per year), erodible lithology and tropical climatic condition. It may be the reason for some indices showing the area to be tectonically less active. These climatic conditions and lithology result in increased erosion. The higher erosion-rate may destroy the evidence of tectonic activity to some extent which affects the result.

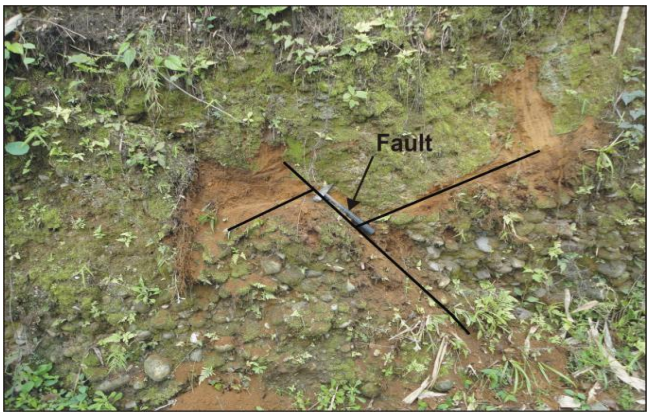

Figure 13: Fault present in tilted terrace deposits.

Figure 14: Strath terrace.


Figure 15: Boulders of the older Subansiri Formation within the Kimin Formation.

According to the Smf index, the area is high to moderately active (Table 2). The degree of tectonic activity in the front H H' and I I' is moderately active. These fronts mark the fault zone of HFT 2 that separates Kimin Formation from Older alluvium. Conditions like heavy precipitation and weak lithology mask the visible tectonic signatures and alter the geomorphic index result. One of the significant geomorphic indexes measured in the mountain fronts is Vf. For Vf calculation, we take the transect distance at 300m and 1 km. The result at 300m brings the valley

Figure. (16) Tilted terraces present in the Harmoti-doimukh road section. (17) The Dikrong River. (18) Harmati Surface (19) Harmati fault scrap.

into a less active class, whereas it is active when measured at a 1 km distance. The Vf value within a drainage basin depends on the valley transect location as the valley becomes progressively narrower upstream in high order drainage basins for a mountain range. A Vf value also depends on the basin area, bedrock lithology and stream discharges (Ramírez-Herrera, 1998). Due to the climatic condition and lithology in the area, the valley erodes at a faster rate. Thus, the index shows the region to be less active.

The Af and T index helps in identifying the tilting direction. The Af and T analysis direct towards the activeness of the area. But the Bs for most of the basins is circular. The basins show circular characteristics due to the high headward erosion of streams because of climate and lithology. The steepness of the mountain fronts helps to find the degree of tectonic activity. The index using this principle is the Mountain Front Steepness Index. The steepness index indicates front I I' more active than HH'. The SL index is one of the most effective tools in finding a zone/point of upliftment or subsidence in a basin. These zone of upliftment/subsidence signify tectonic activity or lithological contact. In the study, the cluster of SL points plotted on the map indicates active tectonics in the area. All the measured geomorphic indexes are used in measuring the index of relative tectonic activity (IRAT). Irat on the calculation, taking Af and SL places the area in an active class. But when calculated with all the parameters, categorize the region into a less active class. Although the result of Irat brings forth that the area has a lesser degree of tectonic activity, the area has an ample number of pieces of evidence and signature that prove the tectonic activeness of the region.

Around the Dikrong River section (Fig. 2), Himalayan Frontal Thrust (HFT) marks the boundary between the alluvium and low hills of Siwalik rocks. There are series of thrust splay branched out from the earlier thrust, and the mountain front propagates along with these thrusts. The bed disposition in the east bank of the Dikrong is steeper than the west bank. There is a differential compression along the east and west bank of the river. This differential compression has led to the development of the NW-SE trending strike-slip fault. Dikrong River (Fig. 17) flows along this strike-slip fault, and it has resulted in the development of an extensional basin with recent sediment deposits.

The ongoing tectonic activity in the area is evident with the rise of the Harmati surface (Fig. 18) above recent alluvium and the presence of fault scrap. In the road section from Harmati to Doimukh on the eastern side of the Dikrong river near the Harmati Tea garden, a fault scrap is present (Fig. 19). It has

raised the terrace deposits over the alluvium along the fault plane of HFT 3. Dasgupta and Biswas, 2000 gave the name Harmati surface to the surface above the scarp. In the NW direction from the Harmati surface, HFT 2 marks the contact between the Kimin Formation and Harmati Surface thrusting Kimin Formation over the Harmati surface. The height of the Kimin Formation at this site is higher than the Harmati surface and increasing in the north direction.

CONCLUSION

The present study includes tectonic activity analysis through geomorphic index assessment such as Smf, Af, T, Bs, SL, Mountain front steepness (S), Vf and Irat. The indices Af, T, SL and S indicate that the area is tectonically active. Several levels of horizontal and tilted, paired, and unpaired terrace deposits are the signature of tectonic activeness. Further, small scale faulting in the terrace deposits and the presence of strath terraces is also evidence of ongoing tectonic activity. So, we can conclude that the area is undergoing tectonic deformation during recent time. But the parameters Smf, Vf and Bs have produced results indicating the region to be moderately or less active. The Irat analysis in this study is calculated separately for Vf measured at two different transect distance that are 300m and 1 km while including all the other parameters. The Irat results put the area in a lesser tectonic activity class (class 4). Also, we calculate Irat taking parameters (SL and Af) that shows high tectonic activity, the result shows the area to be active (class 2).

Some indices indicate the area to be less active. It is because we are following the range of the indexes based on the work in arid and semi-arid climatic condition. The range must vary for the region with tropical to subtropical climatic condition and friable type of sedimentary rock. The high rainfall in the area erodes the mountain fronts and valley width increases where rock resistance is low. Thus, the tectonic activity is not alone in contributing to the alteration of valley shapes and mountain front sinuosity, which affects modification of present morphological characteristics of the area.

ACKNOWLEDGEMENT

We acknowledge the financial support provided to the author by UGC (Basic Scientific Research Fellowship). We are grateful to Prof. Kalpana Deka Kalita, (HOD) Dibrugarh University.

REFERENCES

Allègre, C.J., 34 authors. (1984). Structure and evolution of the Himalaya–Tibet orogenic belt. Nature, 307, 17–19.

Azor, A., Keller, E.A. & Yeats, R.S. (2002) Geomorphic indicators of active fold growth: South Mountain-Oak Ridge anticline, Ventura basin, southern California. Geological Society of America Bulletin, 114, 745–753.

Bezbaruah, D. & Sarma, M. (2013). Morphotectonic Evolution of the Area in and Around Bandardewa, Papumpare District, Arunachal Pradesh. Journal of Earth Science, Special Volume, 223-232.

Bishop, P. (2007). Long-term landscape evolution: linking tectonics and surface processes. Earth Surface Processes Landforms, 32, 329–365.

Bull, W.B. (1977b). Tectonic geomorphology of the Mojave Desert. U. S. Geological Survey Contract Report 14-08-0001-G-394; Office of Earthquakes, Volcanoes, and Engineering, Menlo Park, California, 188.

Bull, W.B. (1978). Geomorphic Tectonic Classes of the South Front of the San Gabriel Mountains, California. U.S. Geological Survey Contract Report, 14-08-001-G-394, Office of Earthquakes, Volcanoes and Engineering, Menlo Park, CA.

Bull, W.B. (2007). Tectonic Geomorphology of Mountains: A New Approach to Paleoseismology. Wiley-Blackwell, Oxford. 328.

Bull, W.B. & McFadden, L.D. (1977). Tectonic geomorphology north and south of the Garlock fault, California. In: Doehring, D.O. (Ed.), Geomorphology in Arid Regions. In Proceedings of the 8th Annual Geomorphology Symposium. (pp. 115-138) State University of New York, Binghamton.

Burbank, D.W. & Anderson, R.S. (2001). Tectonic Geomorphology. Blackwell Science, Oxford, 247.

Cannon, P.J. (1976). Generation of explicit parameters for a quantitative geomorphic study of Mill Creek drainage basin. Oklahoma Geology Notes, 36 (1), 3–16.

Chatterjee, S., Goswami, A. & Scotese, C. R. (2013). The longest voyage: Tectonic, magmatic, and paleoclimatic evolution of the Indian plate during its northward flight from Gondwana to Asia. Gondwana Research, 23, 238–267.

Cox, R.T. (1994). Analysis of drainage-basin symmetry as a rapid technique to identify areas of possible Quaternary tilt-block tectonics: an example from the Mississippi embayment. Geological Society of America Bulletin, 106, 571–581.

Dasgupta, A.B. & Biswas, A.K. (2000). Geology of Assam. Bangalore, Karnataka: Geological Society of India.

Devi, M., Bhakuni, S.S., & Bora, P.K. (2011). Tectonic implications of drainage set-up in the Sub-Himalaya: A case study of Papumpare district, Arunachal Himalaya, India. Geomorphology, 127(1-2), 14-31.

El Hamdouni. R., Irigaray, C., Fernandez, T., Chacón, J. & Keller, E.A. (2008). Assessment of relative active tectonics, southwest border of Sierra Nevada (southern Spain). Geomorphology, 96, 150–173.

England, P. & Molnar, P. (1990). Surface uplift, uplift of rock, and exhumation of rocks. Geology, 18, 1173–1177.

Hack, J.T. (1973). Stream-profiles analysis and stream-gradient index. Journal of Research of the U.S. Geological Survey, 4, 421-429.

Hare, P.W. & Gardner, T.W. (1985). Geomorphic indicators of vertical neotectonism along converging plate margins, Nicoya Peninsula, Costa Rica. Tectonic Geomorphology, 4, 75-104.

Jackson, J., Van Dissen, R. & Berryman, K. (1998). Tilting of active folds and faults in the Manawatu region, New Zealand: evidence from surface drainage patterns. New Zealand Journal of Geology and Geophysics. 41, 377–385.

Karunakaran, C. & Ranga Rao, A. (1979). Status of exploration for hydrocarbons in the Himalayan region- contributions to stratigraphy and structure, Geological Survey of India, Miscellaneous Publication, 41(5), 1–66.

Keller, E.A. (1986). Investigation of active tectonics: use of surficial Earth processes. In: Wallace, R.E. (Ed.), Active tectonics. Studies in Geophysics. National Academy Press, Washington DC, 136–147.

Keller, E.A., Seaver, D.B., Laduzinsky, D.L., Johnson, D.L. & Ku, T.L. (2000). Tectonic geomorphology of active folding over buried reverse faults: San Emigdio Mountain front, southern San Joaquin Valley, California. Geological Society of America Bulletin. 112, 86–97.

Keller, E. A. & Pinter, N. (2002). Active Tectonics: Earthquake, Uplift, and Landscape, (2nd edition), Prentice Hall, New Jersey.

Kunte, S.V., Ganju, J.L. & Datta, N.K. (1983). Geology and structure of the Tertiary belt between Bargang and Pachin Rivers, Arunachal Pradesh. Geological Survey of India, Miscellaneous Publication, 43, 124-129.

Patriat, P. & Achache, J. (1984). India–Asia collision chronology has implications for crustal shortening and driving mechanism of plates. Nature, 311, 615–621.

Pérez-Peña, J.V., Azor, A., Azañón, J.M. & Keller, E.A. (2010). Active tectonics in the Sierra Nevada (Betic Cordillera, SE Spain): Insights from geomorphic indexes and drainage pattern analysis. Geomorphology, 119, 74-87.

Ranga Rao, A. (1983). Geology and hydrocarbon potential of a part of Assam Arakan basin and its adjacent region. Petroleum Asian journal, 1, 127-158.

Ramírez-Herrera, M.T. (1998). Geomorphic assessment of active tectonics in the Acambay Graben, Mexican volcanic belt. Earth Surface Processes and Landforms, 23, 317–332.

Rockwell, T.K., Keller, E.A. & Johnson, D.L. (1985). Tectonic geomorphology of alluvial fans and mountain fronts near Ventura, California. In: Morisawa, M. (Ed.), Tectonic Geomorphology. Proceedings of the 15th Annual Geomorphology Symposium. Allen and Unwin Publishers, Boston, 183–207.

Schumm, S.A., Dumont, J.F. & Holbrook, J.M. (2000). Active Tectonics and Alluvial Rivers. Cambridge University Press.

Silva, P.G., Goy, J.L., Zazo, C. & Bardaji, T. (2003). Fault-generated mountains fronts in southwest Spain: geomorphic assessment of tectonic and seismic activity. Geomorphology, 50, 203-225.

Zovoili E., Konstantinidi. E. & Koukouvelas, I.K. (2004). Tectonic Geomorphology of Escarpments: The Case of Kompotades and Nea Anchialos Faults. Bulletin of the Geological Society of Greece, 36, 1716-1725.

***